EA A Parsimonious Approach to Gravity Inversion for Salt Shape Delineation*

Simone Re[1], Luca Masnaghetti[1], and Elena Medina[1]

Search and Discovery Article #42417 (2019)**
Posted August 12, 2019

*Adapted from extended abstract prepared in conjunction with oral presentation given at 2019 AAPG Annual Convention and Exhibition, San Antonio, Texas, May 19-22, 2019
 DOI:10.1306/42417Re2019

[1]Schlumberger, Milan, Italy (sre@slb.com)

Abstract

In complex salt provinces, the determination of the base of the salt in velocity model building for seismic imaging is a challenging problem even when wide-, rich-, or full-azimuth seismic records are available. Therefore, any additional measurement that can be exploited in order to compensate for the limitation of the seismic illumination represents a valuable tool to mitigate the exploration risks. The purpose of this work is to show how the gravity, and in general potential field data, can be used in an efficient and effective manner in order to reduce the uncertainty in delineating the base of the salt.

Introduction

A principal difficulty with the inversion of gravity data is the inherent non-uniqueness that exists in any geophysical method based upon a static potential field. Since the gravity field is known only on the surface of the earth, there is an infinite number of equivalent density distributions beneath the surface that will reproduce the known field (Li and Oldenburg, 1998). Other than ill-posed, the inversion of the potential field data is also an under-determined inverse problem: the number of observations available is usually far below the number of model parameters that must be estimated. While the intrinsic non-uniqueness of the inversion of potential field data is mitigated by incorporating some a-priori information about the spatial distribution of the property being inferred, the under-determination of the inverse problem can be tackled by reducing the number of parameters to estimate.

An example of a-priori information about the spatial distribution of the property being estimated is the assumption that, due to the isostatic load inducing compaction, the density of the sedimentary package follows a pre-defined mathematical law being, on average, representative of the basin being explored.

The reduction of the under-determination level of the inverse problem, instead, is usually addressed through a careful choice of the property model representation that, in its turn, has usually a direct effect on the number of model parameters that the inverse process must infer.

The most noticeable application of the two techniques mentioned above – i.e. an appropriate use of the a-priori information available and the careful choice of the model representation – is the inversion for the thickness of a sedimentary basin (i.e., depth-to-basement) given the density variation as a function of depth. For this application, there are many examples in literature based on the subdivision of the sedimentary pack into 3D rectangular prisms with depth-dependent density (Cordell, 1973; Chakravarthi and Sundararajan, 2007). Under certain assumptions, the same combination of techniques can be extended to estimate the salt base.

We present an approach based on the decomposition of the salt bodies into 3D rectangular prisms with arbitrary positions in the space and known "top". This technique tries to determine the set of heights of the prisms (i.e., the thickness of the salt bodies) by minimizing the misfit between the observed and the computed gravity anomaly. A synthetic example, loosely based on the Campeche salt province, is used to illustrate the modelling and inversion process, together with its outcomes. The assumptions, the limitations, and the possible ways forward are also discussed.

Superposition and Separation of Effects in the Gravity Signal

Due to the superposition of the effects, the observed gravity anomaly is the sum of all the contributions generated by the different portions of the subsurface. In a gravity survey targeting an offshore salt province - like the synthetic example that will be discussed herein - we can distinguish five geological units that contribute to the total observed anomaly: the mantle, the basement, the sedimentary package, the salt, and the water layer (Figure 1a).

The first step towards the delineation of the salt base through the inversion of the gravity anomaly is the isolation of the signal produced by the density contrast of the salt bodies from the total anomaly.

The effect of the water layer is removed from the observed anomaly as part of the standard data reduction workflow.

The basement and the Moho discontinuity are deep sources of gravity anomaly: due to that, the signal they produce has a low spatial frequency content and this trait can be exploited for inferring their shape. In fact, the Moho and the basement reliefs can be estimated with a pseudo-inverse method, such as the one proposed by Oldenburg (1974) for depth-to-basement estimation, using low-pass version of the observed anomaly.

Once the basement depth has been obtained, it can be used to evaluate, by means of a 3D numerical simulation, the basement contribution to the observed gravity anomaly. With a similar procedure, it is possible to evaluate also the contribution of the density contrast at the Moho and, therefore, the effect of the deep structures can be removed from the observed anomaly by simply subtracting the modelled effects of basement and mantle.

What remains in the reduced observed data after having removed the effects of the water, of the basement, and of the mantle is the anomaly caused by the sedimentary section and by the salt. These two contributions cannot be separated by means of filtering because they overlap in the spatial frequency domain. However, once again, the superposition of the effects can be used to separate the contributions as schematically

explained in Figure 1. Let us assume that the density of the sediments is constant and equal to ρS, that the density of the salt bodies is equal to ρH, and that the sediments are denser than the salt ($\rho S > \rho H$). With reference to Figure 1b, the red curve represents the signal produced by both the sediments and the salt. By subtracting the response of a sedimentary package filling also the space occupied by the salt body (purple curve in Figure 1b), we obtain a residual anomaly (green line) that is caused by a unit that has the same shape of the salt body and a negative density contrast defined as ($\rho H - \rho S$).

Inverse Problem: Formulation and Solution

The residual anomaly produced by the presence of a salt body, computed according to the procedure described above, constitutes the input data for an inverse process that tries to estimate the base of the salt starting from the knowledge of the shape of the top of the salt and the density contrast between salt and sediments.

The inverse process uses a representation of the salt body that is based on its decomposition into rectangular prisms: for sake of simplicity, the decomposition process is schematically depicted in Figure 2a for a two-dimensional salt body. The salt top is represented by the top faces of the prisms, while the unknown salt base consists of the bottom faces of the prisms. Because the depth of the salt top is supposed to be known and fixed, the inversion process operates only on the thickness of the prisms in order to find a salt base that fits the observed anomaly: the thicknesses of the prisms are the model parameters to be inferred by the inversion process. The reasons for the adoption of a prism-based representation are mainly two.

First, the choice of the size of the prisms in the horizontal direction determines the resolution with which the salt top is known and directly controls the number of model parameters that the inversion must infer. On its turn, this provides a strict control on the under-determination level of the problem and allows to counterbalance the intrinsic non-uniqueness of the inversion of potential field data.

Second, the computation of the gravity response of a prism is computationally inexpensive: it is a closed analytic formula if the prism density is constant (Okabe, 1979) and requires only one-dimensional numerical integration if the density changes along the vertical direction (Garcia-Abdeslem, 1992). As already mentioned the size of the prisms along the horizontal directions controls the spatial resolution at which the salt top and the salt base are sampled; therefore, it is crucial to find a trade-off between the level of under-determination of the inverse problem and an adequate level of the lateral resolution of the salt body.

To define the density contrast of each prism, we can assume that the density of the salt is constant while the compaction induced by the isostatic load makes the sediments' density increasing with depth (Figure 3b). This is the reason why, in our formulation we use a salt contrast between salt and sediments that is varying with depth (Saad, 2006). In addition, we do not make any assumption on the mathematical law governing the density increase with depth (e.g. polynomial or exponential): generally, the density of the sediments can be obtained by applying some rock-physics bounded transformation to the compressional velocity field as depicted in Figure 3a. Because of the velocity-density transformation applied, the distribution of the sediments' density changes both horizontally and vertically. The assumption we make, is that

within the volume delimited by a single rectangular prism, the density changes only along the vertical direction. Of course, adjacent prisms can have, and generally will have, different density distributions along depth.

With reference to Figure 2b – and without loss of generality – the vertical attraction g measured by a sensor placed in the origin of a Cartesian system and caused by a prism delimited by $[X_1, X_2]$, $[Y_1, Y_2]$, and $[Z_1, Z_1 + h]$ along the x, y, and z respectively (being γ the gravitational constant) is given by:

$$g = \gamma \int_{Z_1}^{Z_1+h} dz\, \rho(z) \arctan\left(\frac{xy}{z\sqrt{x^2+y^2+z^2}}\right)\Bigg|_{X_1}^{X_2}\Bigg|_{Y_1}^{Y_2}$$

The contribution of a single prism to the total gravity anomaly is then obtained by solving a 1D integral that, from the numerical standpoint, is computed through Gauss-Legendre Quadrature regardless the fact that $\rho(z)$ is a mathematical function or an arbitrary spatial density distribution not following any predefined law.

If the salt body is decomposed into N prisms and the gravity anomaly is recorded at M different points, we can indicate with g_{ij} the vertical attraction caused by the j-th prism at the i-th recording location.

The total vertical attraction at the i-th location is then obtained by summing all the contributions of the N prisms. We want to find the set of thicknesses so that the computed gravity closely matches the observed gravity. A solution to this non-linear inverse problem can be achieved through minimization of a cost function defined as follows:

$$\Phi(\mathbf{h}) = \sum_{i=1}^{M} [d_i - s_i(\mathbf{h})]^2$$

where d_i and s_i are, respectively, the observed and computed anomaly at the i-th location, M is the number of observations, and $\mathbf{h}$ is an N-dimensional vector whose components represent the thickness of the N prisms.

The objective function is minimized iteratively using a Levenberg-Marquardt inversion technique (Pujol 2007). At the k-th iteration, the thickness of the prisms is updated according to the following formula:

$$\mathbf{\Delta h}^k = [\mathbf{A}^T\mathbf{A} + \lambda\mathbf{I}]^{-1}\mathbf{A}^T[\mathbf{d} - \mathbf{s}(\mathbf{h}^{k-1})]$$

where $\boldsymbol{\lambda}$ is a positive scalar quantity, **I** is the identity matrix, and **A** is the sensitivity matrix whose coefficients $\boldsymbol{a_{ij}}$ are, respectively, the derivatives of the of the $\boldsymbol{g_{ij}}$ integrals with respect to the $\boldsymbol{h_j}$ thicknesses.

Synthetic Example

The inversion technique described above was validated on a synthetic data set covering an area of approximately 1050 km^2. The known top of salt (Figure 4a) was sampled using a 400-m spacing along both planar directions leading to approximately 2700 model parameters to be estimated. The residual gravity anomaly (Figure 4b) produced by the salt was computed with a resolution of 600 m along both directions, generating approximately 5000 measurement points.

It is important to remark that the formulation described does not make any assumption neither about the regular sampling of the measure points where the gravity field is recorded nor about the spatial sampling of the salt top and, subsequently, of the salt base. The adoption of a regular spatial sampling step for both data and model parameter was merely dictated by convenience.

The initial salt base was assumed to be flat and located at a depth of 4 km; the initial value of each prism's thickness was computed as the difference between the salt base and the salt top: the inversion process converged in 14 iterations to the solution shown in Figure 5. Figure 5a shows a map view of the percentage error on salt thickness, which is generally good apart from some peaks on salt flanks. The percentage of the data misfit is almost everywhere within 2.5%, as is clearly shown by Figure 5b. A SW-NE section of the true and of the estimated salt bodies overlaid on the density model is depicted in Figure 5c. Finally, Figure 5d and Figure 5e present an example of observed (green line) and predicted anomaly (black line), together with the data misfit (red line) along the same profile of the model section.

Conclusions

We presented a methodology for the delineation of the salt base through an efficient inversion of the gravity anomaly. The methodology is based on two stages. In the first stage, the residual anomaly produced by the presence of the salt is isolated from the total anomaly by exploiting the separation of effects through 3D forward modelling and subsequent effect removal. In the second stage, the residual anomaly is inverted by a process that uses a prism-based representation of the salt body and operates on the prisms' thickness to minimize the misfit between the modeled and the observed data. The technique explained was successfully applied to a real-scale synthetic data set loosely based on the Campeche Basin salt province.

References Cited

Chakravarthi, V., and N. Sundararajan, 2007, 3D Gravity Inversion of Basement Relief – A Depth-Dependent Density Approach: Geophysics, v. 70/2, p. I23-I32. doi.org/10.1190/1.2431634

Cordell, L., 1973, Gravity Analysis Using an Exponential Density-Depth Function-San Jacinto Graben, California: Geophysics, v. 38, p. 684-690. doi.org/10.1190/1.1440367

Garcia-Abdeslem, J., 1992, Gravitational Attraction of a Rectangular Prism with Depth-Dependent Density: Geophysics, v. 57, p. 470-473. doi.org/10.1190/1.1443261

Li, Y., and D.W. Oldenburg, 1998, 3-D Inversion of Gravity Data: Geophysics, v. 63, p. 109-119. doi.org/10.1190/1.1444302

Oldenburg, D.W., 1974, The Inversion and Interpretation of Gravity Anomalies: Geophysics, v. 39, p. 526-536. doi.org/10.1190/1.1440444

Okabe, M., 1979, Analytical Expressions for Gravity Anomalies Due to Homogeneous Polyhedral Bodies and Translations Into Magnetic Anomalies: Geophysics, v. 44, p. 730-741. doi.org/10.1190/1.1440973

Pujol, J., 2007, The Solution of Nonlinear Inverse Problems and the Levenberg-Marquardt Method: Geophysics, v. 72/4, W1-W16. doi.org/10.1190/1.2732552

Saad, A.H., 2006, Understanding Gravity Gradients – A Tutorial: The Leading Edge, v. 25, p. 942-949. doi.org/10.1190/1.2335167

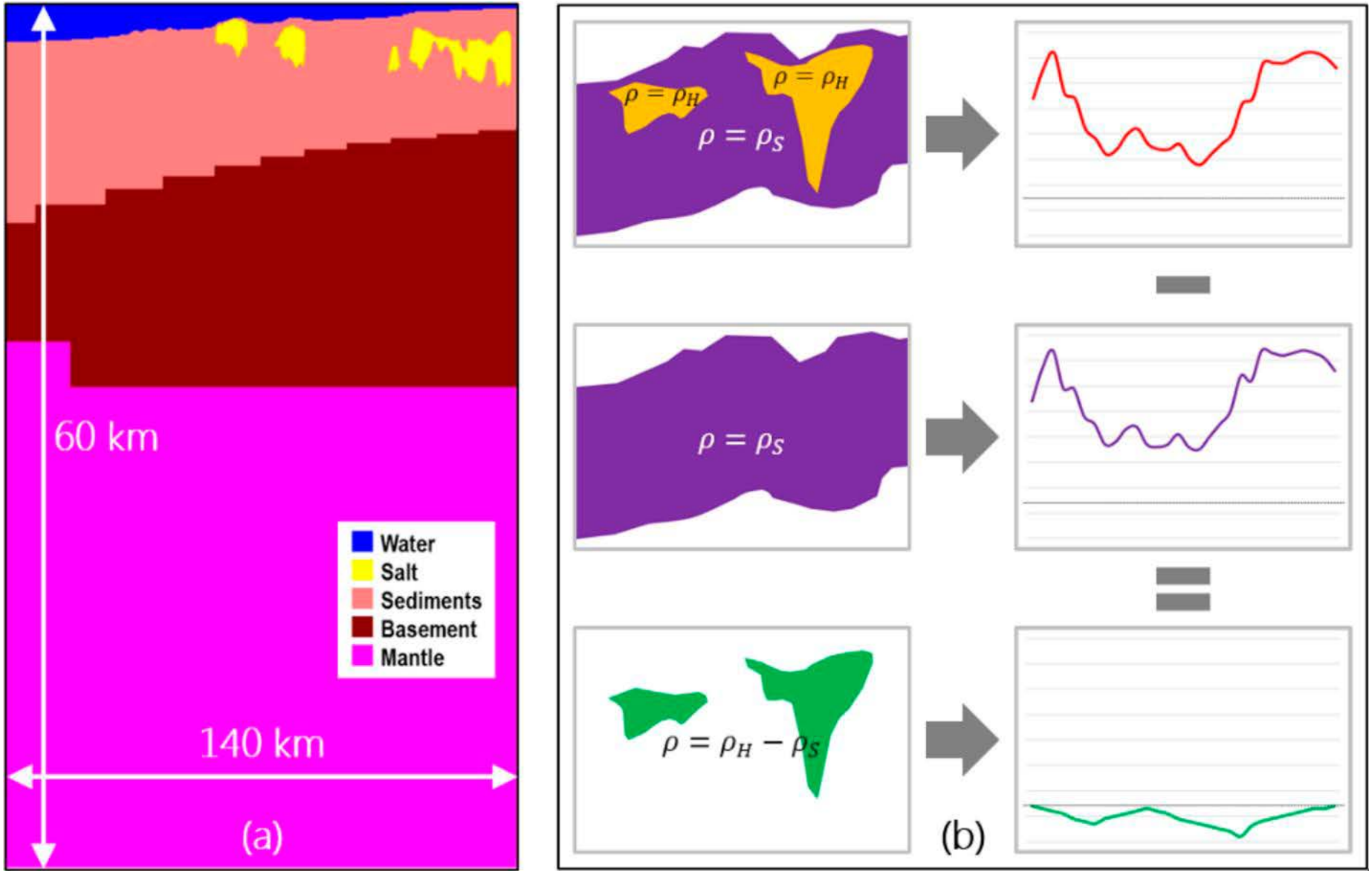

Figure 1. (a) Model section for a realistic marine gravity survey wherein the colors are representative of the various formations contributing to the total gravity anomaly. (b) Graphical explanation of the workflow for isolating the residual gravity anomaly due to salt body.

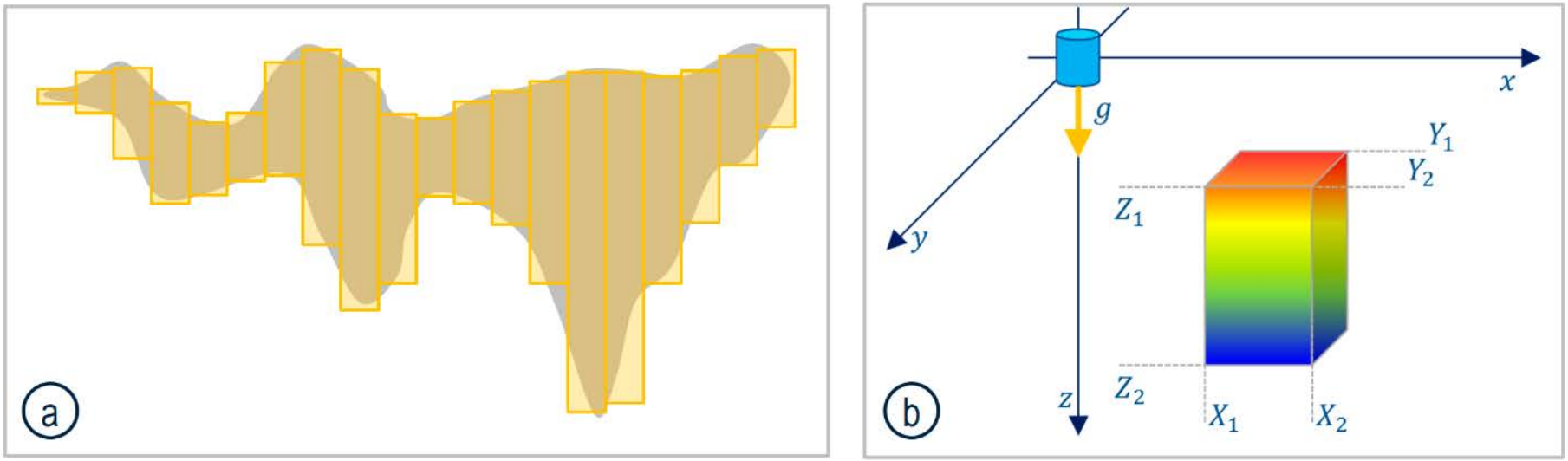

Figure 2. (a) Example of decomposition of a salt body into rectangular prisms. (b) Reference system with the sensor recording the response of the prism with depth-variant density.

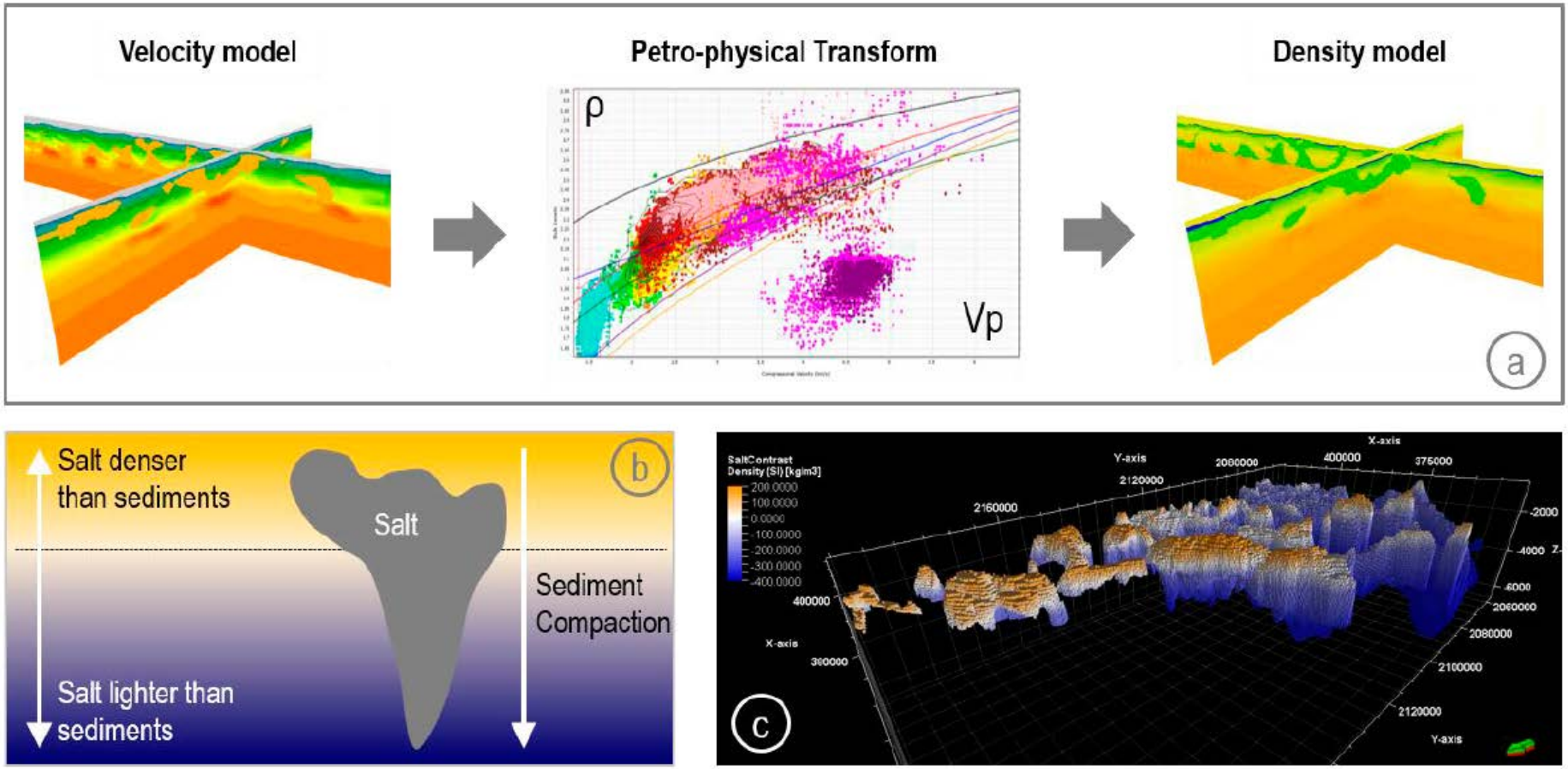

Figure 3. (a) An example of bounded rock-physics transformation that converts the compressional velocity into density. (b) Schematic description of the effect of the compaction on the density contrast between the salt and the surrounding sediments. (c) An example of salt body colored according to the density contrast it produces with respect to the surrounding sediments: the shallow salt is denser than the sediments (positive density contrast, orange) while the deeper salt is lighter than the sediments (negative density contrast, blue).

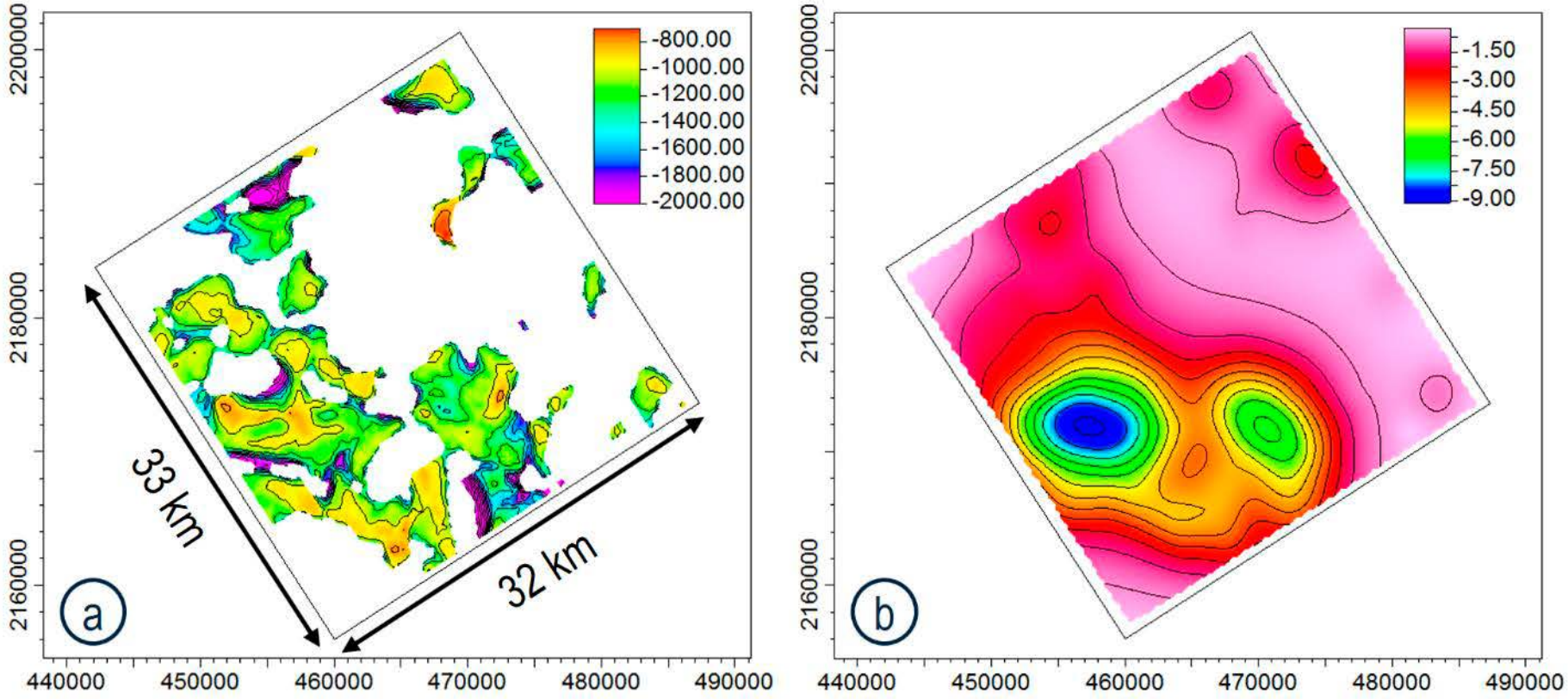

Figure 4. (a) Top of the salt used as input for the inversion. (b) Anomaly produced by the salt body obtained by separation of effects following the procedure described above.

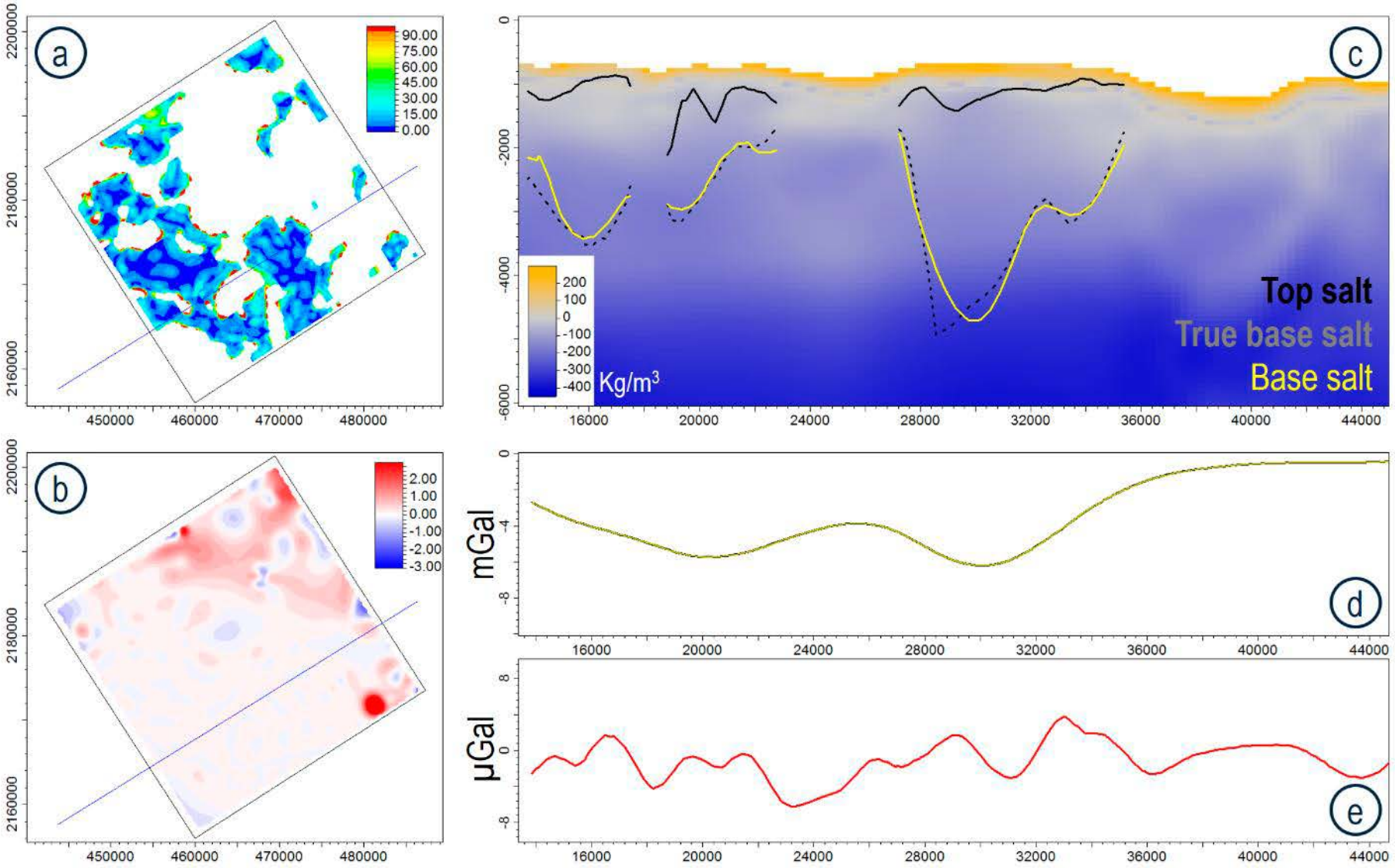

Figure 5. (a) Percentage error on salt-base estimation. (b) Percentage data misfit. (c) Salt top (continuous black line), true salt base (dashed black line), and salt base estimated by the inversion (yellow line) overlaid on density contrast expressed in kg/m³. (d) Observed (green) and predicted (black) gravity data along a profile, in mGal. (e) The data prediction error (red) corresponding to (d), in µGal.